Lipid-mediated interactions tune the association of glycophorin A helix and its disruptive mutants in membranes

Sengupta, Durba; Marrink, Siewert

Published in:
Physical Chemistry Chemical Physics

DOI:
10.1039/c0cp00101e

Publication date:
2010

Lipid-mediated interactions tune the association of glycophorin A helix and its disruptive mutants in membranes

Durba Sengupta* and Siewert J. Marrink

Received 1st April 2010, Accepted 3rd August 2010
DOI: 10.1039/c0cp00101e

The specific and non-specific driving forces of helix association within membranes are still poorly understood. Here, we use coarse-grain molecular dynamics simulations to study the association behavior of glycophorin A and two disruptive mutants, T87F and a triple mutant of the GxxxG motif (G79LG83LG86L), embedded in a lipid membrane. Self-assembly simulations and the association free-energy profile confirm an energetically-favorable dimerized state for both the wild type and the mutants. The reduced association of the mutants compared to the wild type, as observed in experiments, can be justified from comparisons of the free energy profiles. Less-favorable protein–protein interactions as well as disruption of lipid packing around the mutant dimers is responsible for their reduced association. The role of the non-specific "lipid-phobic" contribution appears to be as important as the specific "helix–helix" contribution. However, the differences between the wild type and mutants are subtle and our simulations predict a dimerization state not only for the wild-type glycophorin A, but also for these 'disruptive' mutants. Our results highlight the importance of both specific as well as non-specific driving forces in the association of transmembrane helices, and point to the need of more careful interpretation of experimental measurements.

1. Introduction

Helix association is a key event in membrane protein assembly, occurring usually after the incorporation of the newly synthesized membrane proteins into the lipid bilayer by the translocon machinery.[1,2] Many important bio-energetic and signaling events also involve transient or permanent association of membrane proteins *via* their membrane-spanning domain.[3,4] The structural characteristics of a few such associated transmembrane helices have been determined by X-ray and NMR techniques (see the White-database for protein structures available http://blanco.biomol.uci.edu/Membrane_Proteins_xtal.html). Biophysical techniques have been used in conjunction to investigate the factors responsible for the association of helices in membrane proteins. Helix–helix interactions stabilizing the helix dimer, such as the presence of specific motifs, polar residues and surface complimentary, have been extensively characterized.[5–9] In contrast, the forces driving association, especially the non-specific forces are still poorly understood. The non-specific forces driving helix association include protein–protein (*e.g.* helix-dipole effects), lipid–protein and lipid–lipid interactions.[10] Since most studies on helix–helix dimerization focused on micellar solution, the effect of the surrounding lipids is even less understood though recent studies suggest that the differences between micelles and bilayers may not be as great as previously anticipated.[11] Interestingly, a standard for the dimerization free energy has been proposed only in micelles[12] but not in bilayers.

Groningen Biomolecular Sciences and Biotechnology Institute (GBB) and Zernike Institute for Advanced Materials, University of Groningen, Nijenborgh 4, 9747 AG Groningen, Netherlands. E-mail: s.j.marrink@rug.nl, d.sengupta@rug.nl; Tel: 31 50-3634457

Glycophorin A (GpA) has been the focus of several studies on helix–helix association since it provides a simple and very stable system for understanding the structural basis of helix association (see review[11]). Solution NMR studies in detergent micelles[9] as well as solid state NMR studies[13,14] of the GpA transmembrane dimer showed that it is a right-handed helix pair with a crossing angle of -35°. Several mutagenesis studies coupled with *in vivo* and *in vitro* assays have helped characterize the GxxxG dimerization motif.[8,15–23] Destabilization of the GxxxG motif[20,21] or the polar amino-acid residue T87[18,19,24] have been shown to largely decrease dimerization propensity, and in fact early experimental work using indirect methods to determine the dimer population such as TOXCAT[15] or related assays[20,21] did not detect any dimeric species. However, later studies using more quantitative techniques such as sedimentation equilibrium analytical ultracentrifugation found less-stable dimers with a maximum destabilization of 16 kJ mol^{-1} in disruptive mutants.[18,24] This is probably due to the differences in the definition of a dimer in the two studies, since only closely-packed associated species would give a signal in TOXCAT assays.

The interactions stabilizing the GpA dimer have also been extensively studied in theoretical studies.[25–37] The free energy of association has only been considered in a couple of cases, however. Using an atomistic force field, the potential of mean force (PMF) has been calculated for the association of GpA in dodecanol, a membrane mimetic.[38] No large barriers were observed in the reversible disassociation process and the minimum of the profile was located at a distance separating the centers of mass equal to 0.8 nm. The calculated disassociation free energy was found to be 48 ± 2 kJ mol^{-1}, in good agreement with experimentally determined association constants in detergent solutions. The association free-energy was also

calculated in an implicit membrane model[39] and appears to correlate well to the previous estimate. However, a direct comparison is difficult especially due to the lack of a uniform standard between membranes, membrane mimetics and detergents. Microsecond time-scale coarse-grain simulations of GpA and several mutants[40] have shown that the disruptive mutants were less stable than the wild type, consistent with experimental studies. As yet, the dimerization profile of the GpA within an explicit lipid bilayer has not been calculated probably due to the large computational cost. A comparison of the free-energy profiles of the wild-type GpA with that of its mutants will shed light on the forces driving association of transmembrane proteins.

Here, we use the coarse-grain MARTINI force-field[41,42] to simulate association of GpA and two disruptive mutants, T87F and a triple mutant of the GxxxG motif (G79LG83LG86L), within a dipalmitoyl-phosphatidylcholine (DPPC) membrane. Starting from a disassociated state, we observe spontaneous association of the helices, both wild type and mutants. We also calculate the dimerization profiles (potential of mean force) of the three peptides to justify the experimentally measured differences in association. We further elucidate the role of the lipid-mediated interactions *vs.* specific protein–protein interactions in driving the association of these transmembrane helices.

2. Methods

2.1 Self-assembly simulations

To study the association of glycophorin A (GpA) and its mutants in lipid bilayers, coarse-grained molecular dynamics simulations were performed. The MARTINI force-field (version 2.1)[41,42] was used to describe the peptides, lipids and water. In the MARTINI force-field, a four-to-one mapping is used, *i.e.* on average four atoms and associated hydrogens are represented by a single coarse-grained bead. It has been successfully used to study a variety of peptides and proteins interacting with lipid membranes.[43–46] The current system contained two peptides embedded in a DPPC bilayer of 186 lipids, solvated by 4000 coarse-grained water particles (corresponding to a hydration level of 86 real waters per lipid). Simulations were performed with the wild-type GpA as well as the G79LG83LG86L and T87F mutants. The coarse-grain structures of monomeric GpA was mapped from the atomistic structure of the dimer (PDB code: 1AFO). The two mutants were modeled from GpA by addition of side-chain beads followed by a minimization. All three peptides were modeled as ideal helices, using dihedral potentials to maintain the helicity of the peptides (as described in ref. 42). The inter-helical distance was defined to be the distance between the center of masses of the backbone of the two helices.

The molecular dynamics simulations were performed using the GROMACS software package, version 3.3.1,[47] with the scheme developed for the MARTINI model.[41] The temperature was coupled (coupling time 0.1 ps) to a thermostat at $T = 325$ K using a Berendsen algorithm.[48] The pressure was coupled (coupling time 1.0 ps, compressibility 5×10^{-5} bar^{-1}) using a semi-isotropic coupling scheme, in which the lateral and perpendicular pressures are coupled independently at 1 bar.[48] The non-bonded interactions were treated with a switch function from 0.0 to 1.2 nm for the Coulomb interactions and 0.9 to 1.2 nm for the LJ interactions (pair-list update frequency of once per 10 steps). A time step of 25 fs was used. The simulation times reported in the manuscript are effective times, *i.e.* simulation times multiplied by a factor of four to, approximately, account for the speed-up of coarse-grained dynamics resulting from the neglect of friction associated with the atomistic degrees of freedom.[41,42] Initially, two copies of the monomeric peptide were introduced in a pre-equilibrated DPPC bilayer at a distance of 6 nm from each other. Simulations of 25 μs were performed for each of the three peptides, sufficiently long to observe the self-assembly of GpA and its mutants. The self-assembly simulations were repeated thrice for the wild type and GxxxG mutant and five times for the T87F mutant. Additional simulations with a system twice as large, containing four GpA monomers were also performed.

2.2 Potential of mean force

To compute the PMF between two membrane embedded helices, the same system set-up was used as for the self-assembly simulations. The potential of mean force was calculated using the umbrella sampling technique.[49] The umbrella potential acts on the backbone beads of the first peptide (residue 77–91) with a force constant of 1000 kJ mol^{-1} nm^{-2}. An independent set of simulations with a somewhat lower force constant (800 kJ mol^{-1} nm^{-2}) was performed for the wild type, and resulted in the same PMF profile. For each system (wild type and the two mutants), 21 windows were simulated corresponding to a 0.1 nm shift of the monomer per simulation. The 21 starting structures for each window were created by pulling the two peptides from their associated state, taken from the self-assembly simulation, to their window location using the umbrella potentials with a lower force constant of 500 kJ mol^{-1} nm^{-2} in a 200 ns simulation. Each window was then equilibrated for 200 ns with the full force constant, followed by a 4–8 μs production simulation. The WHAM method[50] was used to unbias the umbrella potentials.

3. Results

To study the association of GpA and its mutants within the membrane, self assembly simulations were performed. Two GpA α-helical monomers were inserted in a parallel orientation into a pre-equilibrated DPPC bilayer with the helices separated at a distance of ≈6 nm. We observed the transmembrane helices to diffuse through the membrane and associate within 5 μs. The self-assembled wild-type dimer packed in a right-handed manner with a negative cross-over angle, fluctuating between −20° and −30°. The helix–helix interface was defined by the residues G79, G83 and T87. The optimum inter-helical distance was 0.75 nm, though a second population with an inter-helical distance of 0.95 nm was also seen. A snapshot of the dimer is shown in Fig. 1 Top. The structure of the self-assembled dimer is consistent with the structures defined by NMR studies[9,13,14] and previous theoretical studies.[27,38,40] Control simulations starting with different initial velocities

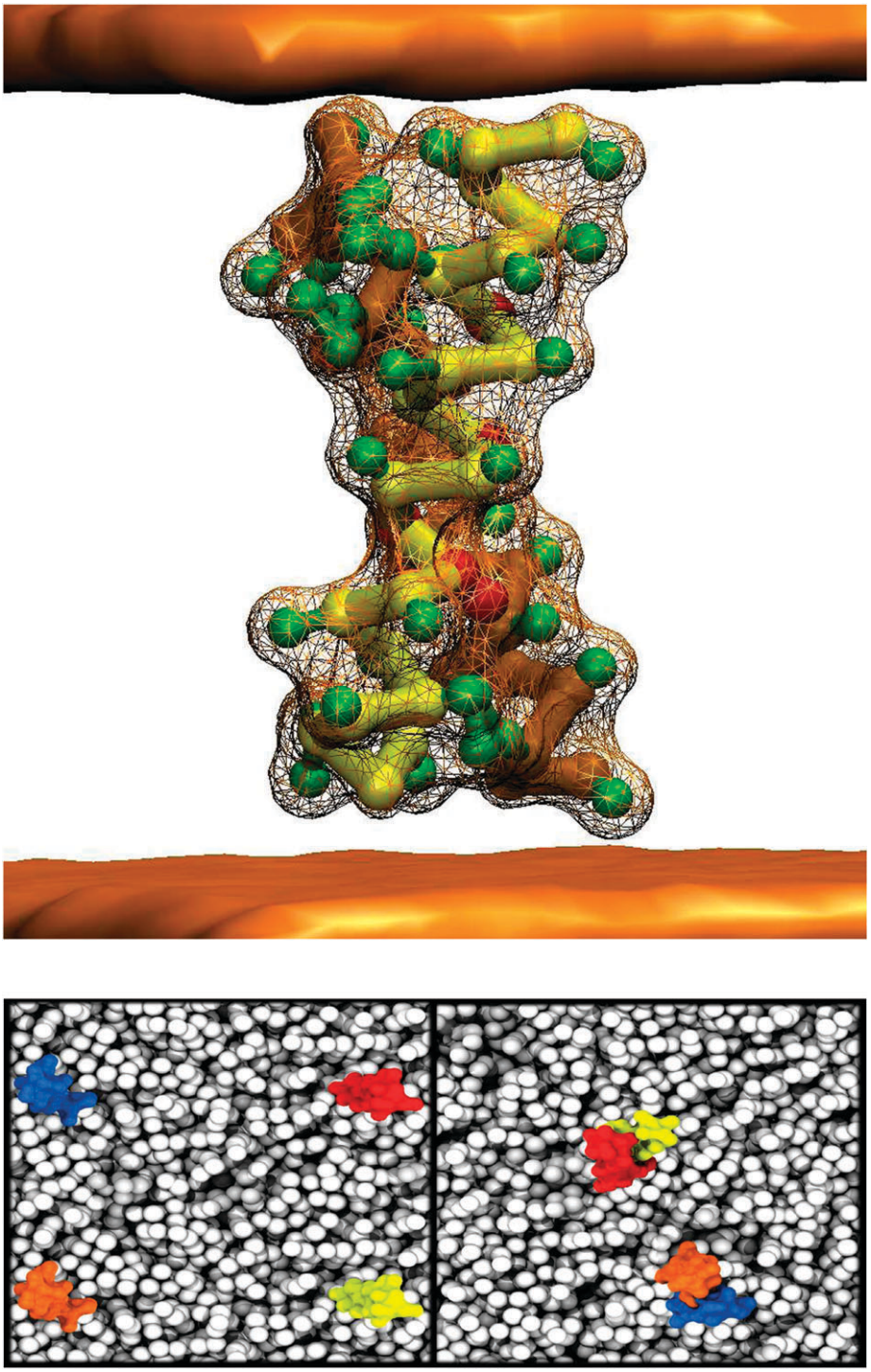

Fig. 1 The coarse-grain representation of the glycophorin A dimer. Top: The backbone beads are shown in yellow and the side chain beads in green. The interface residues (G79, G83, G86 and T87) are highlighted in red. The average phosphate density is shown in orange. Bottom: Top view of the membrane (white) showing the four monomers (depicted in red, blue, yellow and orange) at the start of the simulation (left) and after 1 μs (right), when they associate to form two dimers.

show that the formation and packing of the dimer is reproducible. The time required for association was variable, namely 0.5, 1 and 3 μs in three independent simulations. The time-course of an example simulation is shown in Fig. 2A. No disassociation event was seen in any of the three simulations, each of 25 μs length. The results are consistent with experimental data indicating a strong GpA dimer (see review[11]). To verify the high propensity of GpA monomers to dimerize and not form larger non-specific aggregates, we simulated a larger system (four monomers in a simulation box). In three independent simulations, the monomers self-assembled within 5 μs to form two dimers (see Fig. 1 Bottom).

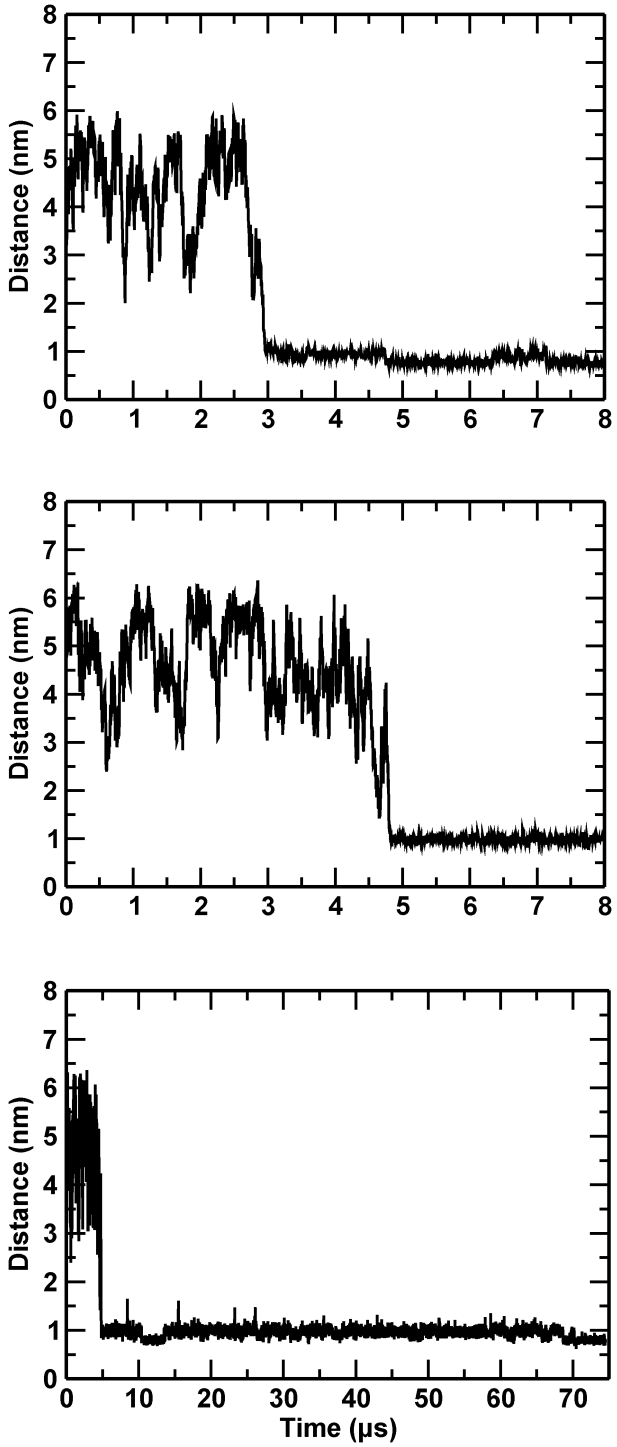

Fig. 2 Time-course of the inter-helical distance. (A) The distance between the monomers of the wild-type GpA, simulation wt-1. (B) The distance between the monomers of the T87F mutant, simulation m1-1. (C) Extension of simulation m1-1, showing the distance between the T87F mutant monomers.

3.1 Disruptive mutants of GpA also associate, albeit to non-native structures

We also simulated self-assembly of two disruptive mutants: a point mutant T87F and a triple mutant (G79LG83LG86L) disrupting all three glycines involved in the dimerization motif. Five independent simulations were performed for the T87F mutant and three for the triple mutant. Similar to the wild type, the transmembrane helices of the T87F mutant were observed to associate on a time scale between 2 and 5 μs (an example is shown in Fig. 2B). The dimers formed were stable but the structure was different with respect to the structure of the wild type. The average inter-helical distance of the dimerized species was 1.0 nm (T87F), larger than that of the wild type (0.85 nm). Different helix–helix interfaces were sampled, accompanied by a large spread of cross-over angles ranging between -30° and 30°. The dimer appeared to be less well packed although no dissociation events were seen in any of the five 25 μs simulations. One simulation was extended even further (to 75 μs), but the peptides remained as a dimer (Fig. 2C). Surprisingly, the triple mutant, mutating the entire GxxxG motif, also associated in the membrane on time-scales of 1–3 μs. Similar to the T87F mutant, a wide range of interfaces and cross-over angles was sampled and the average inter-helical distance is 0.95 nm. Again, the dimers remained associated during the entire 25 μs, in three independent simulations. The optimum inter-helical distance of the two mutants, 0.9 nm (T87F) and 0.85 (GxxxG), are also larger than that of the wild type (0.75 nm).

The self-assembly simulations point towards a favorable associated state for both the wild-type GpA and its two disruptive mutants, though at different inter-helical distances. However, even at a μs time-scale, it is difficult to sample the dissociated state in the simulation box.

3.2 The dimerization profile of GpA shows two deep minima and no barriers to association

To analyze the difference in the energy between the associated and dissociated state of the three peptides, we calculated the dimerization free energy profile, or potential of mean force (PMF). The PMF of the GpA dimer is shown in Fig. 3 Top. The free-energy of the two well separated monomers is assumed to be zero. The minimum in the profile is located at a distance separating the centers of mass equal to 0.75 nm, corresponding to the associated state sampled in the self-assembly simulations. As the two TM segments of GpA move away from each other, the free-energy increases and a second minimum, less deep than the first, is seen at a distance separating the centers of mass equal to 0.9 nm. As the separation of the α-helices further increases, the free-energy rapidly increases and the profile levels off and reaches a plateau at approximately 20 nm, a distance beyond which the dimer is fully dissociated. A third local minimum can also be discerned at around 1.2 nm. This minimum corresponds to the regime just before lipid-separated helices. After this point, at inter-helical separations larger than 1.4 nm, the helices are separated by at least one lipid molecule.

The PMF profile shown in Fig. 3 Top was calculated from twenty one windows, each simulated independently for 8 μs (totaling 168 μs). The long time-scales were required since adequate sampling was not achieved with shorter times. At the shorter time-scales, sampling was inadequate for helix–helix separations larger than the native-like starting structure. To illustrate the importance of long sampling times, the PMF

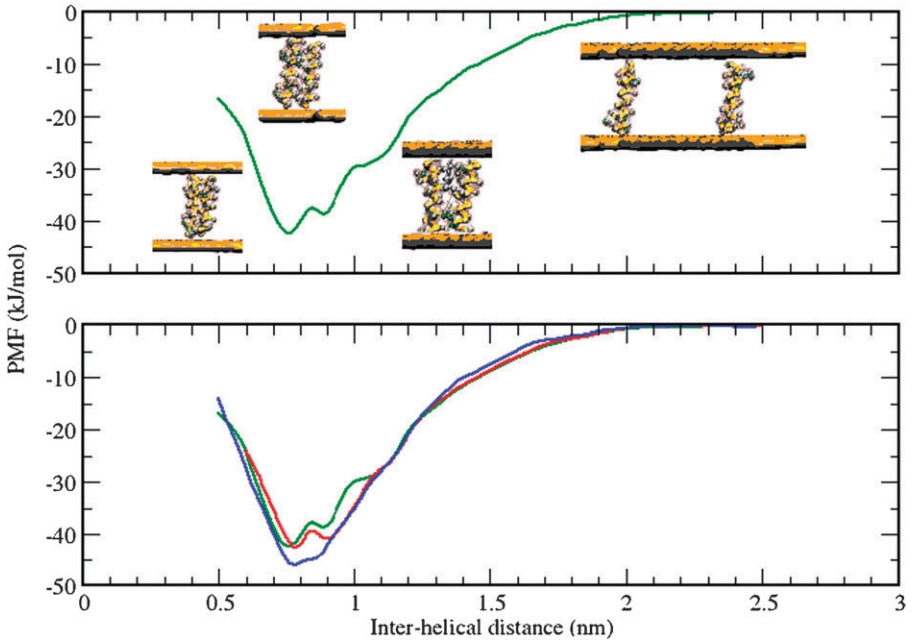

Fig. 3 The potential of mean force of GpA, calculated by umbrella sampling calculations at a sampling of 8 μs (green), 4 μs (red) and 0.5 μs (blue) sampling per window.

profiles calculated taking into account only the first 0.5 μs or 4 μs are shown in Fig. 3 Bottom. Although the global shape of the profile is already sampled using 0.5 μs sampling per window, the second minimum only becomes apparent after prolonged sampling. Thus, only the native wild-type dimer state, which was the starting structure, was sampled initially, and it takes much longer to sample a variety of non-native but associated structures (see also next section). Increasing the sampling in each window to up to 8 μs leads to a convergence in the PMF profile.

The free-energy difference between the fully-separated state and the dimerized state is $\approx 40 \pm 4$ kJ mol^{-1}. The apparent dissociation free energy ΔG^{dis} can be obtained by integrating the PMF profile $G^{\mathrm{PMF}}(r)$ to an appropriate separation, which delineates the limit of association. In cylindrical coordinates, the association constant can be written as[38]

$$K_a = \pi \int_0^{\lambda_{\max}} \lambda \exp[-\beta G^{\mathrm{PMF}}(\lambda)] \mathrm{d}\lambda \qquad (1)$$

Here, $\lambda_{\max}$ stands for the cylindrical radius separating associated and dissociated states of the two α-helices and is taken to be 2.5 nm. The integral reaches a plateau beyond 1.8 nm and the value of K_a is not sensitive to that of $\lambda_{\max}$. The apparent dissociation free energy is then given by $\Delta G^{\mathrm{dis}} = -RT\ln(K_a)$. Numerical integration of eqn (1), using the PMF profile as depicted in Fig. 3 Top, results in $\Delta G^{\mathrm{dis}} = 38.2$ kJ mol^{-1} for the wild-type GpA.

3.3 Native and non-native associated states of GpA contribute to the different minima

To analyze the species contributing to the three minima in the PMF (Fig. 4A), the average inter-helical crossing angle as a function of the reaction coordinate was calculated (Fig. 4B). The profile can be divided into three regimes. Below 0.8 nm, the crossing angle remains close to the native angle averaging −25°. In the second regime, corresponding to a separation of up to 1nm, a large spread in cross-over angles is seen, both native-like right-handed as well as non-native left-handed cross-over angles are sampled (see Fig. 4C, solid line). The second regime corresponds to the second minimum seen in the PMF. At separations larger than 1.5 nm, the average cross over angle is zero, indicating that at large distances, the helices keep the orientation characteristic of the monomer.

3.4 The disruptive mutants also show a minimum and no barriers during association

The PMF of disassociation was also calculated for the T87F and the GxxxG mutant. A comparison of the PMFs with that of the wild type is shown in Fig. 5. The dimerization profile is similar to the wild type and the minimum of the PMFs for both the mutants is at the associated state. The mutants also show no barriers to association and point towards free association within the membrane. However, the two mutants can not approach as closely as the wild-type GpA; at distances below 1.0 nm the PMF increases rapidly and the minimum corresponding to the native-like structure is missing. The other two regimes seen in the wild type are present: the less well-packed minima with a large spread in cross-over angle and a lipid-separated dimer. The exact value of the inter-helical distance in the three regions may vary (within 0.02 nm) for the three species (wild-type and mutants) but the structural characteristics in the different regions are similar. The difference in energy between the fully-separated and the dimerized helices is 30 kJ mol^{-1} for the GxxxG mutant and 28 kJ mol^{-1} for the T87F mutant (*cf.* 40 kJ mol^{-1} for the wild-type). Using eqn (1), the dissociation free energy is calculated to be 30.2 kJ mol^{-1} for the GxxxG mutant and 27.8 kJ mol^{-1} for the T87F mutant (*cf.* 38.2 kJ mol^{-1} for the wild-type). Thus,

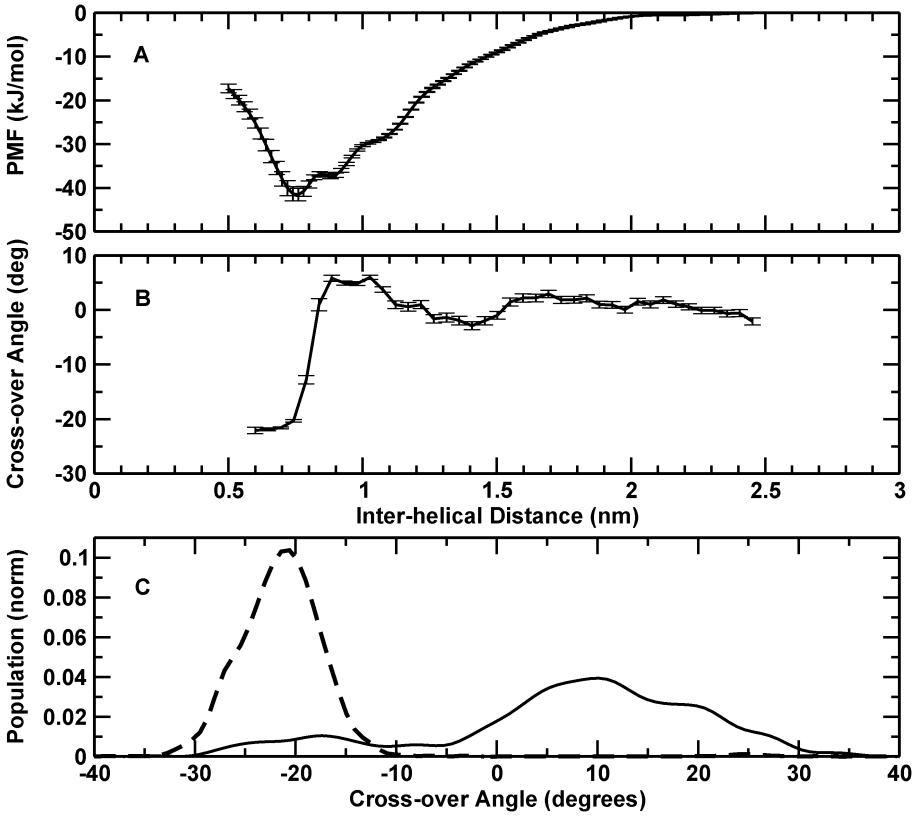

Fig. 4 The PMF (A) and cross-over angle (B) as a function of inter-helical distance for GpA. (C) Populations of the cross-over angles at inter-helical distances less than 0.8 nm (dashed line) and between 0.8 and 1.0 nm (solid line).

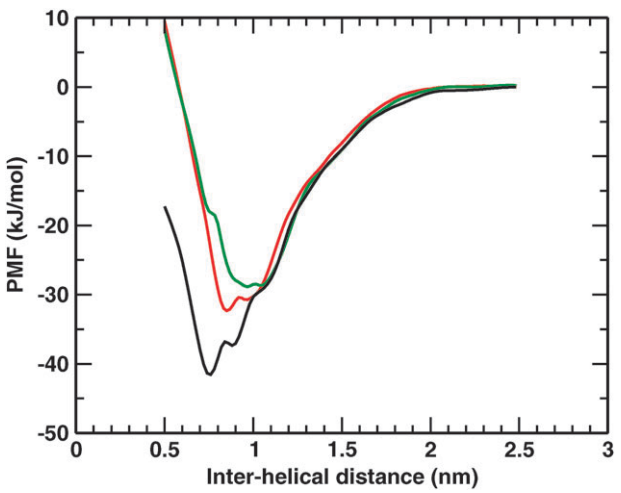

Fig. 5 PMF of wild-type GpA (black), T87F mutant (green) and GxxxG mutant (red).

the mutants have a lower free-energy of association compared to the wild type, corresponding to a destabilization of 8 kJ mol^{-1} for the GxxxG mutant and 10.4 kJ mol^{-1} for the T87F mutant.

3.5 Association of dimers is driven by both helix and lipid packing

To shed some light on the driving forces of the strong dimerization of GpA, we analyzed the helix–helix, lipid–lipid and helix-lipid interaction terms (Fig. 6). The global minimum in the helix–helix interaction energy (for both back-bone beads—Fig. 6A as well as all beads—Fig. 6B) is located around 0.6–0.7 nm, at slightly smaller distance compared to the global minimum in the PMF. At larger separations, the energy increases with increasing separation. Beyond $\sim$1.5 nm the helices do not interact at all (note that the coarse-grained force field only considers pair interactions within a 1.2 nm cut-off). The second minimum seen in the PMF does not correspond to a local-minimum in helix–helix association. From Fig. 4, we see that this regime comprises of an ensemble of structures with a spread in cross-over angles, sampling both native and non-native states. Therefore, we suggest that the second minima is mainly due to the entropic contribution of the large high-energy conformational space available to the non-native states and the multiple packing states for the side-chains associated with these non-native states.

The lipid–lipid energy term also decreases as the helices approach each other and shows a minimum when the helices are dimerized. Interestingly, an increase in the energy is seen when the helices approach each other closer than the native distance, indicating a disruption of the lipid packing around the "super-packed" GpA dimer. The disruption of lipid packing around the dimer is probably due to the pointing outwards of the terminal bulky residues when the helices approach each other closer than the native inter-helical distance. The flipping out of the side-chain residues leads to a disruption of lipid packing compared to ideal values at native distances. A minimum is also seen around 1.3 nm,

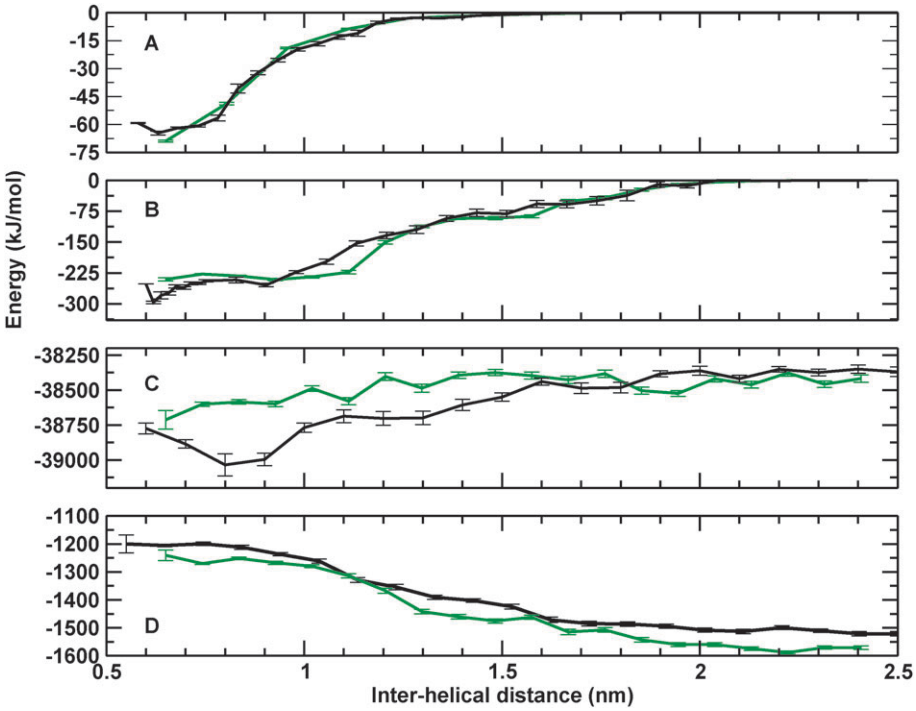

Fig. 6 The driving force of association: (A) Helix–helix interaction energy (backbone only), (B) Helix–helix interaction energy (all beads), (C) Lipid–lipid energy, (D) Helix-lipid interaction energy for the wild-type GpA (black) and T87F mutant (green).

corresponding to the third local minimum in the PMF, just before the lipid-separated regime. Thus implying that the third minimum in the disassociation profile is due to lipid–lipid interactions.

To understand the cause of the decreased association of the mutants, the interaction energies were again calculated. Not surprisingly, the helix–helix interaction (back-bone only) is similar for the wild-type peptide and its mutants (Fig. 6A). However, the contributions from the side-chains is significant. The helix–helix interaction (all beads) for the T87F mutant is shown in Fig. 6B and compared to the wild-type. A single flat minimum up to 1 nm is seen and the minimum at low inter-helical distances (0.8 nm) is absent. Also, the helix–helix interaction energy is higher than the wild-type. In both cases, the interaction energy is zero above an inter-helical distance of 2 nm. Surprisingly, the largest difference in interaction energies between the wild-type and mutant is the contribution of the lipid–lipid term. The lipid–lipid energy term for both the wild-type and mutant is shown in Fig. 6C. Similar to the wild-type, as the helices approach each other in the mutant, the interaction between the lipids is increased. However, the decrease in the interaction energy between the lipids is not as favorable as in the wild-type and a large difference in energy is observed at low helix–helix distances.. Thus, the packing of the lipids around the mutant is significantly altered compared to the wild-type. The well-defined minimum seen at the native-like inter-helical distance for the wild-type is also absent in the mutant. The helix–lipid interaction energies are lower for the mutant compared to the wild-type but followed the same trend (see Fig. 6D). Thus, not just is the packing of the helices disturbed in the mutant but also the packing of the lipids around the helices. The two factors together contribute to the decreased association seen in the mutants of GpA.

4. Discussion

Using the MARTINI force-field we were able to simulate the self-assembly of the GpA dimer, embedded in a DPPC membranes, to its native-like structure. In the simulations, once the monomers associated, no disassociation events were seen, consistent with experimental results indicating a strong dimer (see review[11]). Interestingly, also two disruptive mutants were observed to dimerize, with no subsequent disassociation events seen on a multi-microsecond time scale. Analysis of the free energy profiles, however, reveal that the mutant dimers are less stable compared to the wild-type, by about 8–10 kJ mol^{-1}, mainly as a result of less efficient helix–helix packing and a larger disruption of the lipid membrane surrounding the dimer state. The results we obtain for the wild type and the T87F mutant are in contrast to a previous study using a related force-field in which disassociation events were seen.[40] Although we do not understand the origin of this apparent discrepancy, we point out that the current results are obtained with a more thoroughly calibrated version of the Martini force field. Using the same version of the force-field as in the current study, multiple disassociation events have been observed for WALP peptides in disordered membranes (unsaturated PC lipid enriched domain), indicating a much lower affinity for association compared to the disruptive mutants of glycophorin A (L. Schaefer *et al.*, in preparation). It is also important to stress the long simulation times required to obtain convergence for the free energy profiles. We showed that microsecond simulation times are required to remove correlation to the starting structure and to obtain accurate binding free energies. In order to validate our results, it is important to compare to experimental measurements and results obtained with more detailed (all-atom) simulation models.

The association free energy calculated for the wild-type, 38.2 kJ mol^{-1}, cannot directly be compared to experimental measurements that are typically performed on micellar systems. No standard method exists to compare the associations in the two systems though it has been proposed to compare only the hydrophobic volume in lieu of the total volume.[12,39] In this case, we relate our apparent standard of the number of protein molecules in the volume of the membrane, to the standard proposed in micellar systems which is number of moles of protein in the micellar volume, which does not include the aqueous phase. The standard free energy of dimerization can then be written as: $\Delta G_{\mathrm{micelle}} = \Delta G_{\mathrm{bilayer}} + RT\ln\left(\frac{2}{N_A^2 V}\right)$, where N_A is Avogadro's constant and converts the apparent standard of the number of molecules in our simulation box to the number of moles and V is the volume of the membrane (in liters) and relates to 1M hydrophobic volume of the micellar system. Adopting this standard, the conversion of the value to a "detergent-like" standard state gives -29.2 kJ mol^{-1}. The value calculated is comparable to previous standardized estimates of association free energy in C_8E_5 (-30 kJ mol^{-1})[12] and C_{12} maltoside micelles (-32 kJ mol^{-1}).[23] Both experiments and simulations thus point to a strongly bound dimer in case of the wild-type GpA.

This is also apparent from the calculated PMF for dimerization, revealing two important features: a deep minimum for the bound state and lack of a barrier to association. The depth of the minimum as well as the absence of barriers is very similar to the PMF calculated previously in a membrane mimetic at atomistic resolution.[38] A small local minimum around helical separation of 1.2 nm is seen in both studies corresponding to the regime just before the solvent-separated helices. With longer sampling, a second minimum (absent at lower time-scales) at longer inter-helical distances was seen in our calculations, but not in the short time-scale atomistic study. This state corresponds to non-native states. Analysis of the energetic contributions furthermore revealed that the driving forces of association are a combination of favorable helix–helix and lipid–lipid interactions upon dimerization.

Perhaps somewhat surprisingly, we found that the two disruptive mutants also have a strong tendency to associate within the membrane. We estimate a $\Delta\Delta G$ of 8 kJ mol^{-1} for the G79LG83LG86L (GxxxG) mutant and 10.4 kJ mol^{-1} for the T87F mutant. The values are similar to those measured by ultracentrifugation methods for the G79L, G83L and T87L mutants (10–14 kJ mol^{-1}).[18] However, the results are in contrast to earlier studies using biochemical and genetic assays. It had been long established that in the disruptive mutants (*e.g.* T87A) either no dimer fraction can be detected[19] or they have a large value of $\Delta\Delta G$ (16 kJ mol^{-1} measured by TOXCAT assay).[24] However, using ultra-centrifugation methods, $\Delta\Delta G$ of only 4.2 kJ mol^{-1} was measured for the same mutant (T87A).[16,18] The TOXCAT assay is based on the activation of transcription of the reporter gene (CAT) by the ToxR domains when brought together by the transmembrane domains. We speculate that perhaps the four-fold difference in $\Delta\Delta G$ is partly due to the larger inter-helical distances being unable to position the ToxR domains in the required distance and orientation. Furthermore, ultracentrifugation measurements showed that the $\Delta\Delta G$ of the double mutants (16.8 kJ mol^{-1} for the G79LG83L mutant) is less than the addition of the single mutants (25.2 kJ mol^{-1}).[17] Thus, even disruptive mutants, long believed to not dimerize, may associate in membranes.

The PMF for the mutants was similar in shape to that of the wild-type, with no barrier to association. The position of the minimum was at larger inter-helical distances (0.95 nm for T87F, 0.85 nm for GxxxG compared to 0.75 nm for the wild-type), and in fact is at a similar position as the second minimum seen in the wild type PMF. Apparently only the wild-type can optimize its helix–helix interactions specifically, resulting in very close packing. In contrast, the dimer state for the mutants corresponds to non-specific aggregates. Evaluation of the driving forces also underline this difference; both helix–helix interactions and lipid–lipid contributions to the association energy are lower for the mutants compared to the wild-type. The results indicate that the bulkier mutants disrupt both their own packing as well as packing of the surrounding lipids.

Our results point to a significant contribution of lipid packing in modulating dimerization in GpA and its mutants. The role of the lipid as a non-specific driving force appears to be as important as the specific "helix–helix" contribution. The contribution of lipid packing to membrane-protein folding and association has been discussed but not assessed experimentally and contradictory theoretical estimates are found in the literature.[51–53] We could also not correlate the large decrease in lipid packing contribution directly with a proportional change in the surface-area (hydrophobic/hydrophilic) of the mutants, indicating that the contribution could be more complex than can be estimated with simple models. The specificity of GpA to form dimers and not higher order aggregates points towards a critical balance between the specific and non-specific forces. To fully understand the energetics of association within the membrane, the role of lipids in modulating association needs to be explored further.

An additional feature of interest of the dimerization of GpA in the membrane is the apparent universality of the association profile. The profile calculated here at a coarse-grain level of description in a DPPC bilayer matches the profile calculated at atomistic description in a dodecanoyl slab.[38] The similarity between the profiles is remarkable since both the environment and the level of description differ in the two studies. The disassociation of two pVNVV peptides, model peptides based on the GCN4 leucine-zipper, in DMPC membranes has also shown a remarkably similar profile.[54] Using a very coarse-grained description of a generic peptide in a bilayer, it has furthermore been shown that such a dimerization profile could be characteristic of single transmembrane domains[55] in general. Even peptides not expected to associate, such as WALP peptides, have been shown to associate within membranes,[10] albeit with a lower propensity than glycophorin A. It appears that association of single helix domains in the membrane, driven by the non-specific forces, could be more prevalent than expected. We speculate that the lipid–phobic forces drive single helices to associate within the membrane into non-specific aggregates but packing into well-packed dimers requires specific helix–helix interactions. The association

of larger membrane proteins appears to be less favorable and involves an energy barrier that would prevent non-specific associations.[55] To tune transient associations of single helices in the membrane, such as signaling peptides, interaction with other proteins or lipids are probably required. The *in vivo* association state of single transmembrane receptors that have been a paradigm for monomeric peptides, has also been questioned such as for the erythropoietin receptor[56] where it was suggested that the receptors exist as loosely-associated species, assembling into well-packed species only in the presence of a trigger such as ligand binding. In fact, the proposed signalosomes point towards the direction that receptor aggregates could be more commonly found than monomeric receptors. It would be important to calculate the association profiles of other single-helix proteins to discern barriers and calculate association constants to be able to understand and possibly tune such protein clusters within membranes.

5. Conclusions

Based on an extensive set of coarse-grained simulations of the glycophorin-A dimer in an explicit membrane environment, we conclude that both wild-type GpA and two mutants (T87F and GxxxG) form stable dimers. The association is driven by a combination of indirect lipid–phobic forces and direct helix–helix interactions. Both contribute to a relative stabilization of about 8–10 kJ mol^{-1} of the wild-type dimer compared to the dimer formed by the disruptive mutants. Only the wild-type dimer is well packed, corresponding to the native state observed in NMR experiments. The mutants associate into a less specific aggregate characterized by larger packing distance and multiple binding modes. Differences between wild-type and mutant peptides only become apparent at microsecond time scales, pointing to the importance of long sampling times. We further note that the two main characteristics of the dimerization free energy profile obtained for GpA, namely a deep minimum and absence of significant barriers to association, is also observed in other simulation studies, and conclude that it may describe transmembrane helix–helix dimerization in general.

References

1 S. H. White and G. von Heijne, *Curr. Opin. Struct. Biol.*, 2004, **14**, 397–404.
2 C. A. Woolhead, P. J. McCormick and A. E. Johnson, *Cell*, 2004, **116**, 725–736.
3 M. Mellado, A. J. Vila-Coro, C. Martinez and J. M. Rodriguez-Frade, *Cell Mol. Biol.*, 2001, **47**, 575–582.
4 J. Schlessinger, *Cell*, 2000, **103**, 211–225.
5 C. Choma, H. Gratkowski, J. D. Lear and W. F. DeGrado, *Nat. Struct. Biol.*, 2000, **7**, 161–166.
6 F. X. Zhou, H. J. Merianos, A. T. Brunger and D. M. Engelman, *Proc. Natl. Acad. Sci. U. S. A.*, 2001, **98**, 2250–2255.
7 R. M. Johnson, C. L. Heslop and C. M. Deber, *Biochemistry*, 2004, **43**, 14361–14369.
8 M. A. Lemmon, H. R. Treutlein, P. D. Adams, A. T. Brünger and D. M. Engelman, *Nat. Struct. Biol.*, 1994, **1**, 157–163.
9 K. R. MacKenzie, J. H. Prestegard and D. M. Engelman, *Science*, 1997, **276**, 131–133.
10 E. Sparr, W. L. Ash, P. V. Nazarov, D. T. S. Rijkers, M. A. Hemminga, D. P. Tieleman and J. A. Killian, *J. Biol. Chem.*, 2005, **280**, 39324–3933.
11 K. R. MacKenzie and K. G. Fleming, *Curr. Opin. Struct. Biol.*, 2008, **18**, 412–419.
12 K. G. Fleming, *J. Mol. Biol.*, 2002, **323**, 563–571.
13 S. O. Smith, M. Eilers, D. Song, E. Crocker, W. Ying, M. Groesbeek, G. Metz, M. Ziliox and S. Aimoto, *Biophys. J.*, 2002, **82**, 2476–2486.
14 S. O. Smith, D. Song, S. Shekar, M. Groesbeek, M. Ziliox and S. Aimoto, *Biochemistry*, 2001, **40**, 6553–6558.
15 W. P. Russ and D. M. Engelman, *Proc. Natl. Acad. Sci. U. S. A.*, 1999, **96**, 863–868.
16 K. G. Fleming and D. M. Engelman, *Proc. Natl. Acad. Sci. U. S. A.*, 2001, **98**, 14340–14344.
17 A. K. Doura and K. G. Fleming, *J. Mol. Biol.*, 2004, **343**, 1487–1497.
18 A. K. Doura, F. J. Kobus, L. Dubrovsky, E. Hibbard and K. G. Fleming, *J. Mol. Biol.*, 2004, **341**, 991–998.
19 M. A. Lemmon, J. M. Flanagan, H. R. Treutlein, J. Zhang and D. M. Engelman, *Biochemistry*, 1992, **31**, 12719–12725.
20 B. Brosig and D. Langosch, *Protein Sci.*, 2008, **7**, 1052–1056.
21 D. Langosch, B. Brosig, H. Kolmar and H. J. Fritz, *J. Mol. Biol.*, 1996, **263**, 525–530.
22 I. Mingarro, P. Whitley, M. A. Lemmon and G. von Heijne, *Protein Sci.*, 1996, **5**, 1339–1341.
23 L. E. Fisher, D. M. Engelman and J. N. Sturgis, *Biophys. J.*, 2003, **85**, 3097–3105.
24 M. T. Duong, T. M. Jaszewski, K. G. Fleming and K. R. MacKenzie, *J. Mol. Biol.*, 2007, **371**, 422–434.
25 A. Elofsson and G. v. Heijne, *Annu. Rev. Biochem.*, 2007, **76**, 125–140.
26 H. R. Treutlein, M. A. Lemmon, A. T. Engelman and D. M. Brunger, *Biochemistry*, 1992, **31**, 12726–12732.
27 P. D. Adams, D. M. Engelman and A. T. Brunger, *Proteins: Struct., Funct., Genet.*, 1996, **26**, 257–261.
28 J. A. G. Briggs, J. Torres and I. T. Arking, *Proteins: Struct., Funct., Genet.*, 2001, **44**, 370–375.
29 T. Lazaridis, *Proteins: Struct., Funct., Genet.*, 2003, **52**, 176–192.
30 D. G. Metcalf, P. B. Law and W. F. DeGrado, *Proteins: Struct., Funct., Bioinf.*, 2007, **67**, 375–384.
31 L. Bu, W. Im and C. B. III, *Biophys. J.*, 2007, **92**, 854–863.
32 W. Im, M. Feig and C. B. III, *Biophys. J.*, 2003, **85**, 2900–2918.
33 J. M. Cuthbertson, P. J. Bond and M. S. P. Sansom, *Biochemistry*, 2006, **45**, 14298–14310.
34 H. I. Petrache, A. Grossfield, K. R. MacKenzie, D. M. Engelman and T. B. Woolf, *J. Mol. Biol.*, 2000, **302**, 727–746.
35 R. Braun, D. M. Engelman and K. Schulten, *Biophys. J.*, 2004, **87**, 754–763.
36 M. Mottamal, J. Zhang and T. Lazaridis, *Proteins: Struct., Funct., Bioinf.*, 2006, **62**, 996–1009.
37 E. Psachoulia, M. D. P, P. J. Bond and M. S. P. Sansom, *Acc. Chem. Res.*, 2010, **43**, 388–396.
38 J. Hénin, A. Pohorille and C. Chipot, *J. Am. Chem. Soc.*, 2005, **127**, 8478–8484.
39 J. Zhang and T. Lazaridis, *Biophys. J.*, 2006, **91**, 1710–1723.
40 E. Psachoulia, P. W. Fowler, P. J. Bond and M. S. P. Sansom, *Biochemistry*, 2008, **47**, 10503–10512.
41 S. J. Marrink, H. J. Risselada, S. Yefimov, D. P. Tieleman and A. H. de Vries, *J. Phys. Chem. B*, 2007, **111**, 7812–7824.
42 L. Monticelli, S. K. Kandasamy, X. Periole, R. G. Larson, D. P. Tieleman and S. J. Marrink, *J. Chem. Theory Comput.*, 2008, **4**, 819–834.
43 X. Periole, T. Huber, S. J. Marrink and T. P. Sakmar, *J. Am. Chem. Soc.*, 2007, **129**, 10126–10132.
44 S. Yefimov, P. Onck, E. van der Giessen and S. J. Marrink, *Biophys. J.*, 2008, **94**, 2994–3002.
45 M. Fuhrmans, V. Knecht and S. J. Marrink, *J. Am. Chem. Soc.*, 2009, **131**, 9166–9167.
46 D. Sengupta, A. Rampioni and S. J. Marrink, *Mol. Membr. Biol.*, 2009, **26**, 422–434.
47 D. van der Spoel, E. Lindahl, B. Hess, G. Groenhof, A. E. Mark and H. J. C. Berendsen, *J. Comput. Chem.*, 2005, **26**, 1701–1718.

48 H. J. C. Berendsen, J. P. M. Postma, W. F. van Gunsteren, A. D. Nola and J. R. Haak, *J. Chem. Phys.*, 1984, **81**, 3684–3690.
49 G. M. Torrie and J. P. Valleau, *J. Chem. Phys.*, 1977, **23**, 187–199.
50 S. Kumar, J. M. Rosenberg, D. Bouzida, R. H. Swendsen and P. A. Kollman, *J. Comput. Chem.*, 1992, **13**, 1011–1021.
51 V. Helms, *EMBO Rep.*, 2002, **3**, 1133–1138.
52 D. R. Fattal and A. Ben-Shaul, *Biophys. J.*, 1993, **65**, 1795–1809.
53 P. Lagüe, M. J. Zuckermann and B. Roux, *Biophys. J.*, 2000, **79**, 2867–2879.
54 J. Lee and W. Im, *J. Am. Chem. Soc.*, 2008, **130**, 6456–6462.
55 F. J. M. de Meyer, M. Venturoli and B. Smit, *Biophys. J.*, 2008, **95**, 1851–1865.
56 S. N. Constantinescu, T. Keren, M. Socolovsky, H. S. Nam, Y. I. Henis and H. F. Lodish, *Proc. Natl. Acad. Sci. U. S. A.*, 2001, **98**, 4379–4384.

